CONCURRENT ENGINEERING APPLICATION IN MICROSYSTEM TECHNOLOGY

NICOLAE TANASE[1], GABRIELA IOSIF[1*], ADRIAN NEDELCU[1], IULIAN IORDACHE[1], ANA-MARIA LUCHIAN[1], GEORGE SUCIU[2], VICTOR SUCIU[2], EMIL COSTEA[3]

Abstract. _The concurrent engineering is a modern design concept through which the product manufacture is safety accomplished. The flow chart illustrates the essential contributions which avoid the start mistakes and correct connection with market. The application of this design procedure brings important advantages: the primary manufacturing stages are fully automated, a unitary approach of item production, a minimal spent design time, a real-time connection between the contributing departments, a correct view of market supply._

Keywords: _Microelectromechanical system, concurrent engineering, numerical simulation._

1. INTRODUCTION

The microsystems technology can become more efficient by correct implementing the concurrent engineering. The primary manufacturing stages are fully automated and promote generalized institutional collaboration. An illustration of the information flow in concurrent engineering relative to the traditional model for achieving the product is presented in Figure 1. As can be seen, there are significant time savings when concurrent engineering is implemented in the design-manufacturing cycle of the product realization. Also, concurrent engineering method does not lead to implementation problems of the manufacture design [1]. Fundamentally, in concurrent engineering, the product manufacturing responds to the requirement of expert involvement by interconnection in the design stage, which represents a new concept.

Once the design team completes all the activities, the production processes are based on product design. Concurrent engineering allows the promotion of innovations accepted by all emerging design factors, as well as the elimination of errors from the launch of the new product idea.

It can be noticed that while the design method by concurrent engineering starts by having the quality and the cost of the product as main purposes, the traditional method does not have such a reference. After the design stage, the concurrent engineering team compares the resulting cost of the product project with the target cost. The production of any item may begin only when the estimated cost is less or equal than the target cost. Such a design discipline is essential to ensure that the price of the product is competitive on the market. A typical model of concurrent engineering for product manufacture is shown in Figure 2.

---

[1] INCDIE ICPE-CA, 030138 Bucharest, Romania. E-mail: gabriela.iosig@icpe-ca.ro.
[2] BEIA CONSULT INTERNATIONAL, 041386 Bucharest, Romania.
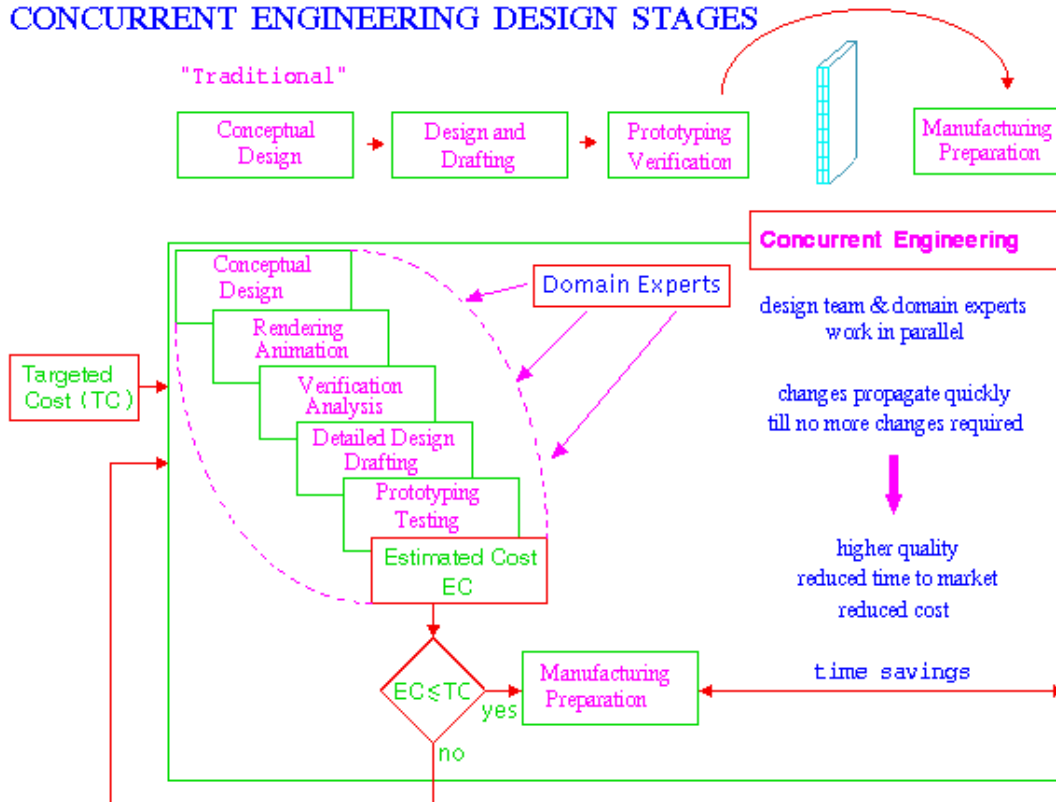[3] INCAS, 061126 Bucharest, Romania.

Figure 1. Design stages in concurrent engineering [1].

The model of concurrent engineering is based on an expert team that is responsible for the entire product life cycle from the initial idea to the finite product. Such a accomplishment team brings together the design, engineering and manufacturing expertise [1].
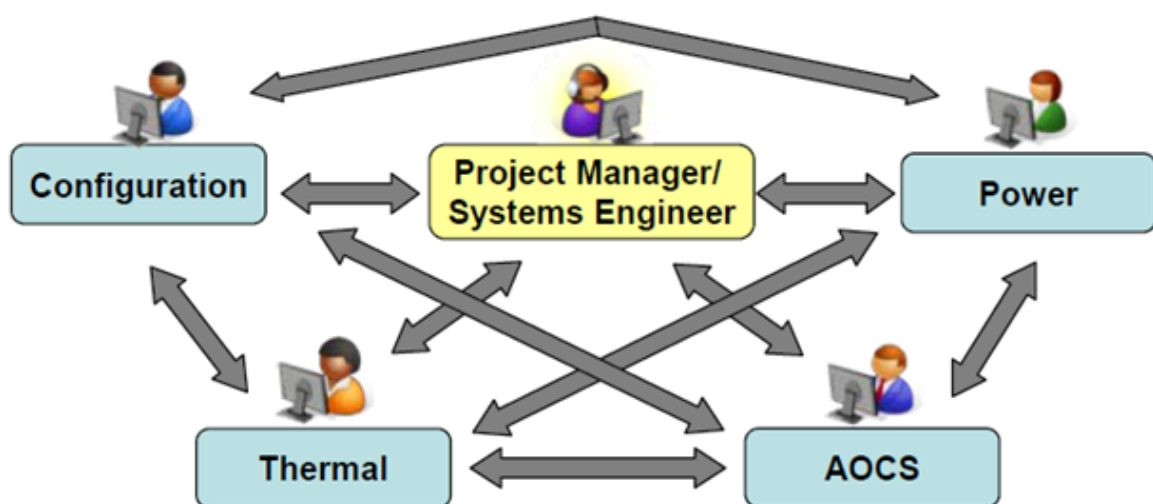

Figure 2. Concurrent Design/Engineering Processes.

In concurrent engineering, the market analysis stage defines the new ideational product strategy in terms of market requirements and suggests the targets of the sales price and of the production cost, objectives that become inputs into the "design wheel".

The marketing department usually initiates new product ideas. Such ideas are based on market research, after studying customer needs.

The marketing department is not totally independent in conducting this marketing study. In the design flow configuration, various other departments contribute with useful information such as the production capacity of a certain product proposal, and help the marketing department to formulate a more accurate idea for a new product. Finally, the idea is presented to the design team that has design purposes and objectives defined more clearly. An essential outcome of the marketing analysis is to set the sale price and the target of production costs [1] .

A defining characteristic of concurrent engineering is that, by product design, concurrent engineering team design the process at an early stage of manufacture; the team decides what kind of equipment will be used, the layout of the machines, etc. (Fig. 3).
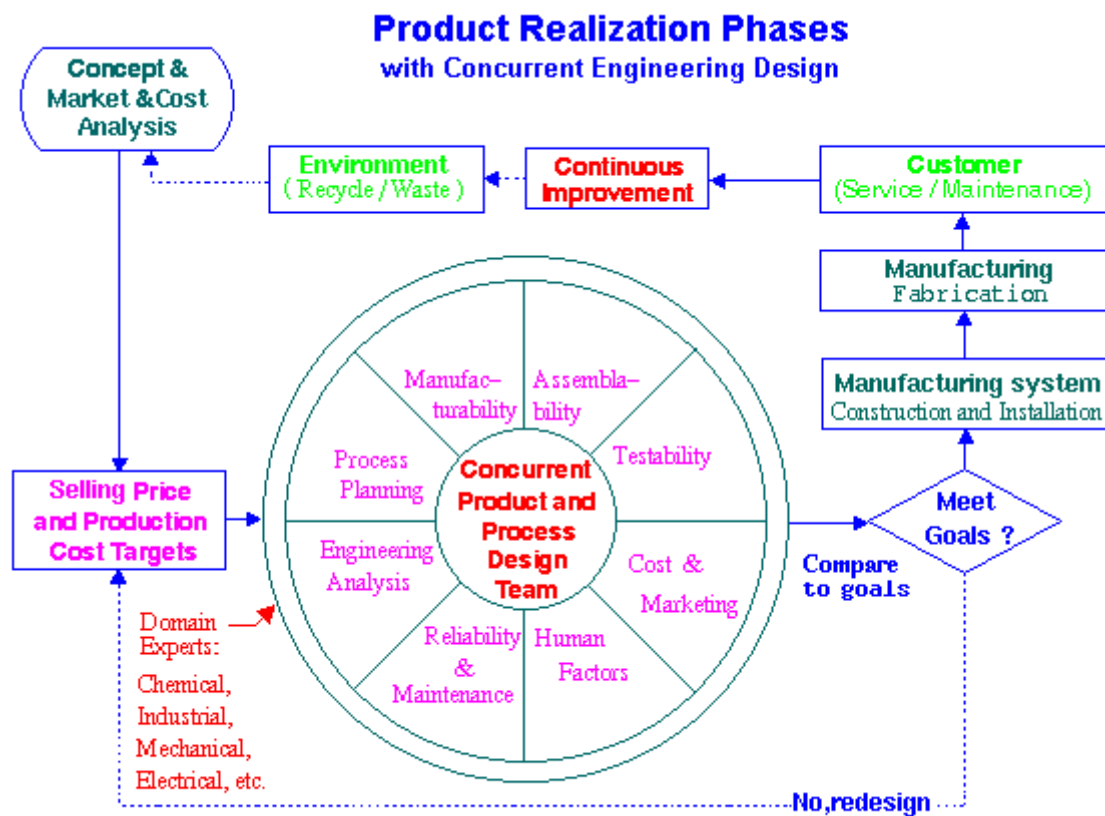

Figure 3. Stages of product realization using concurrent engineering design – adapted from H. R. Parsaei et al. [1, 2].

2. IMPLEMENTATION ANALYSIS OF CONCURRENT ENGINEERING IN THE MANUFACTURE OF A MICROACTUATOR

MEMS (Microelectromechanical Systems) magnetic systems present a new class of micro devices with great applicative potential. Using the same technology as conventional MEMS applications and incorporating magnetic materials as a sensitive element, but also as

an actuator element, new possibilities are offered and new markets are opened in the fields of information technology, automotive, biomedical, aerospace and instrumentation. MEMS magnetic systems are based on electromagnetic or magnetic interactions from magnetic materials and active electromagnetic coils or passive magnetic fields, such as permanent magnets. Magnetic materials can be deposited on micro-components and assembled into micro-devices.

In this paper the experimental and numerical simulation results, but also modelling results are presented underlying a concurrent engineering cycle, as well as the manufacturing technologies for magnetic motion microactuators of cantilever type system BCMS (*bending-mode cantilever microactuators*). This type of BCM is designed either to reflect an incident laser beam for an accurate positioning of it, or to create a microscanner.

The paper presents the modelling of a bi-directional magnetic actuator cantilever beam BCM type, whose 3D model was designed using a specialized CAD software SolidWorks Office Premium 2014, which allows parameterized design of the electromechanical products, thus resulting the virtual 3D model of the optimized BCM microactuator, required for experimental simulations. Furthermore, the results obtained in this paper will be validated in the project E-STAR [17], where the coordinator ICPE-CA and partners INCAS and BEIA developed concurrent engineering platform architecture for processing big data on cloud platforms.

MEMS magnetic devices with permanent magnets has benefits due to the constant energy stored in hard magnetic materials, which leads to reduced energy consumption; Also they have small dimensions and a simple electronic circuit as compared to an electromagnetic actuator with variable reluctance. The limited number of electromagnetic actuators in MEMS is partly due to the manufacturing difficulties of the electromagnetic micro actuators using silicon-based MEMS technology, and partly due to some misconceptions about electromagnetic drive. In addition to the commercial use of hard magnets, only a few microdisks use these permanent magnets [2-5], compared to many MEMS magnetic devices that use thin magnetic layers.

Microelectromechanical (MEMS) systems based on magnetic interactions between magnetic materials and electromagnetic coils are used in microactuation because they offer various advantages as compared to the electrostatic and piezoelectric actuators in terms of power consumption, polarity and deactivation. These advantages also include the generation of long-radius forces and deviation with low command voltage, even in severe operating conditions. For example, they can be used in intelligent laser technology applications used in fluorescence-based cellular measurement systems, pressure and vibration sensors, bidirectional microsensors, semi-cylindrical mirrors with variable focal point and correction of aberrations (spherical and chromatic characteristics), *etc*.

In this paper a basic concept for concurrent engineering is presented regarding a cantilever beam type actuator that is provided with a matrix of permanent magnets at the free end of an elastic blade, which is made of a polyimide (super) paramagnetic material (PI) type. Alternatively, the blade can be made of non-magnetic material (permanent or temporary), but in this case a Permalloy type plate is inserted between the magnets and the blade.

The magnets interact with the magnetic field produced by the electric current that circulates through a spiral, planar and excitation coil, placed on a silicon-based support plate. Figure 4 presents the two constructive variants that have been analysed. The electric current is adjustable, and it provides the adjustment of the flexible plate deflection from PI (Polyimde) [6-7].
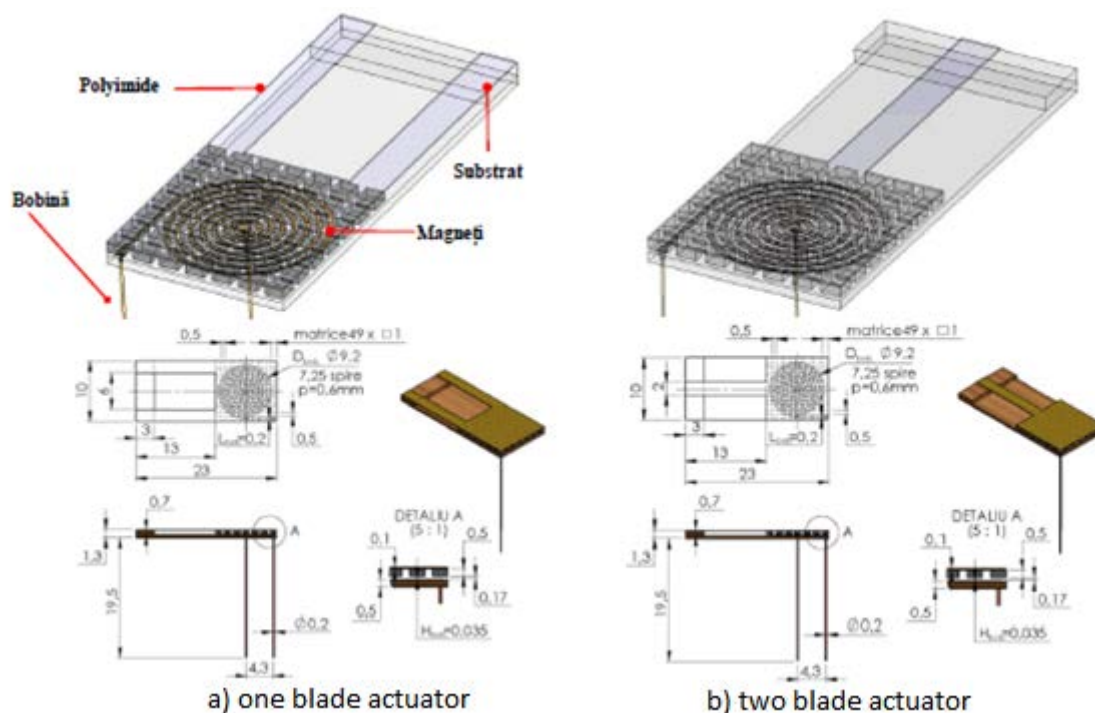
Figure 4. 3D CAD design of a bending cantilever mode (BCM) microactuator.

3. RESULTS AND DISCUSSION

The numerical simulation is carried out on 3D computing domains. The concurrent engineering approach requires solving some interdependent problems of stationary and magnetic-stationary electric field, but also of materials strength. The electric field generating electric current together with the permanent magnets represents magnetic field source, when the electro-dynamic forces acting on the actuator system occur.

Mathematical models describing physical phenomena are interconnected in one 'sense' - the magnetic field does not change the distribution of electric current in the coil, and the structural deformations do not change the magnetic field distribution in the system. In order to consider the coupling magnetic field-elastic mechanical structure in both directions, the use of deformable mesh networks is required in numerical solving.

This study also includes a structural modal analysis that allows the determination of the first six (structural) own actuator frequencies and of the associated deformations.

In the first stage of design, the problem of the electro-kinetic field for the distribution determination of the conduction electric current density distribution in the coil must be solved. Then the problem of the magnetic field (the determination of the volume magnetic force) arises and, in the third stage, the structural problem is integrated. For FEM solution of the electro-kinetic problem Lagrange square elements were used, linear vector elements were used for the magnetic field, and also for deformations Lagrange square elements were used [7].

3.1. IMPORT OF THE 3D CAD MODEL, THE PROPERTIES OF MATERIALS AND THE ADDITION OF THE INITIAL PARAMETERS

The substrate of the actuators is made of silicon, the windings are made of copper, the elastic blades are made of polyimides (PI), and the permanent magnets are NdFeB type [6-9]. The PI has a lower elastic modulus E, which allows a large deflection angle. Table 1 lists the structural properties for BCM parts.

Table 1. Electrical, magnetic and mechanical properties of the actuator components [7].

Material	E [GPa]	ν	ρ_{st} [kg/m^3]	μ_r	B_r [T]	s_r	σ [S/m]
PI (cantilever)	2.94	0.35	1410	1	-	3.4	6700
Silicon (support)	170	0.28	2329	1	-	12.1	-
Copper (PSC coil)	110	0.35	8700	1	-	1	5.998e7
NdFeB (Matrix of permanent matrix)	150…245	0.26	8720	1,1	1,2-1,4	1.05	7.143e5

Fig. 5 shows the model designed in the SolidWorks 2014 Professional software that was exported in the STEP data transfer format for 3D import into the Comsol Multiphysics 5.0 computing program, which solves the simulations presented in the following chapters.
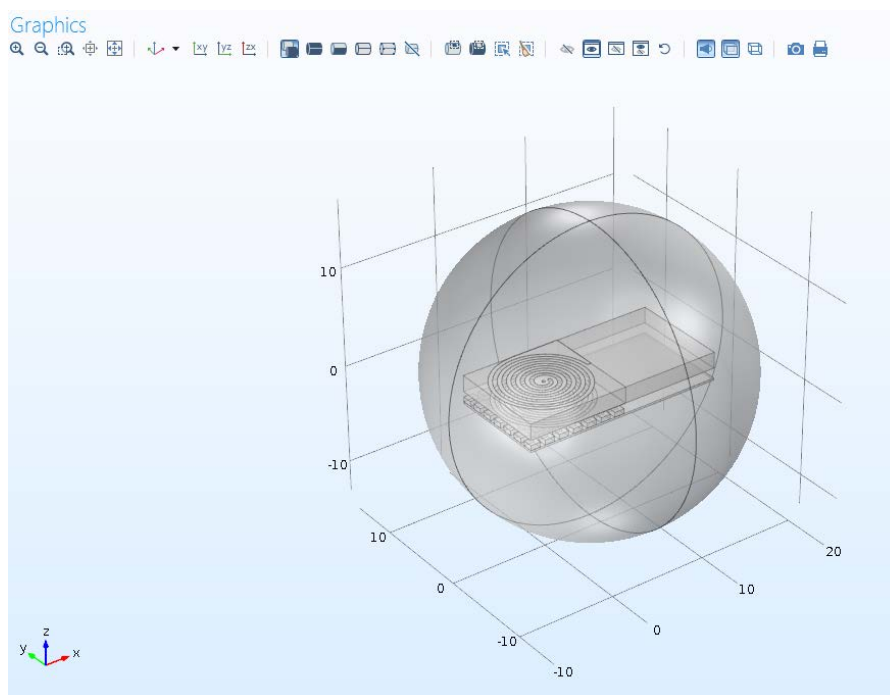

Figure 5. Import of the 3D CAD model created in SolidWorks 2014.

The magnets are oriented with the residual induction **B**r in the *xOy* plane parallel to the *Ox* axis. It is assumed that the interface between them and the PI blade is a (super) paramagnetic foil for which $\mu_r = 10$ was assumed. Its presence is modelled by assigning the magnetic properties of the foil to PI blade. A more detailed analysis of this interface (permeability, size) and of the permanent magnets arrangement will be made in the next stage.

The magnetic field produced by the permanent magnets interacts with the magnetic field produced by the operating current, resulting a force that produces the deformation of the PI blades. This force must be repulsive. The deformation of the blades is analyzed under stationary working conditions.

3.2. SOLVING THE COUPLED SIMULATION (ELECTRO-KINETIC FIELD, MAGNETIC FIELD, STRUCTURAL PROBLEM)

First, the problem of the electromagnetic field is solved and then using the electromagnetic field data, the structural analysis is solved based on the results of the electromagnetic field problem as input data for the mechanical problem. First order vector elements were used for the magnetic field and second order Lagrange elements for electro-kinetic and structural problems [8,9], [13], [15,16].

The mathematical model:

a) Stationary electromagnetic field model:

b)

$$\nabla \cdot \left(\sigma_{el} \nabla V \right) = 0 \tag{1}$$

$$\nabla \times \left(\mu_0^{-1} \mu_r^{-1} \nabla \times \mathbf{A} - \mathbf{B}_r \right) = \mathbf{J} \tag{2}$$

$$\mathbf{f}_{EM} = \nabla \cdot \overline{\overline{T}}_{EM} \tag{3}$$

where: $\mathbf{A}$ – vector magnetic potention[T m], $\mathbf{J}$ – current density [A mm^{-2}], $\mathbf{f}_{EM}$ - electromagnetic force [N m^{-3}], $\overline{\overline{T}}_{EM}$ - tensor of the magnetic moment (Maxwell)

b) Structural model:

$$\mathrm{d}V/\mathrm{d}V_0 = \rho/\rho_0 = \det\left(\mathbf{F}\right) \tag{4}$$

$$\overline{\overline{C}} = \mathbf{F}^T \mathbf{F} - \mathbf{I} \tag{5}$$

$$\varepsilon = \frac{1}{2}\left(\overline{\overline{C}} - \mathbf{I} \right) = \frac{1}{2}\left(\mathbf{F}^T \mathbf{F} - \mathbf{I} \right) \tag{6}$$

$$\overline{\overline{\sigma}}_{st} = E\overline{\overline{\varepsilon}} \tag{7}$$

where: $\mathbf{F}$- elongation gradient, $\overline{\overline{C}}$ - Cauchy-Green tensor (right), ε- Green elongation, $\overline{\overline{\sigma}}_{st}$- symmetric tensor of Cauchy elongations

3.3. SOLVING THE ELECTRIC FIELD PROBLEM. DEFINITION OF THE INITIAL CONDITIONS FOR THE ELECTROMAGNETIC FIELD PROBLEM

In order to solve the electromagnetic field problem, using simplifying elements of geometry and operation, the following stages related to the physical and geometrical modeling are completed (Fig. 6).

The physical modeling, in which starting from the analysis of the device functioning principle and from the identification of the main phenomena and causal relationships (internal and external causes of the field), simplifying physical assumptions of the analysis and implicitly the electromagnetic field regime are set and the main physical characteristics that characterize the operation of the analyzed device are identified, making assumptions about how they vary in time and space; the geometrical modeling aims to identify the computing field and subfields that are relevant for this problem, by analyzing the spatial symmetries and variations of the problem, the spatial domain size is determined (1D, 1.5D, 2D, 2.5D, 3D) and its shape.
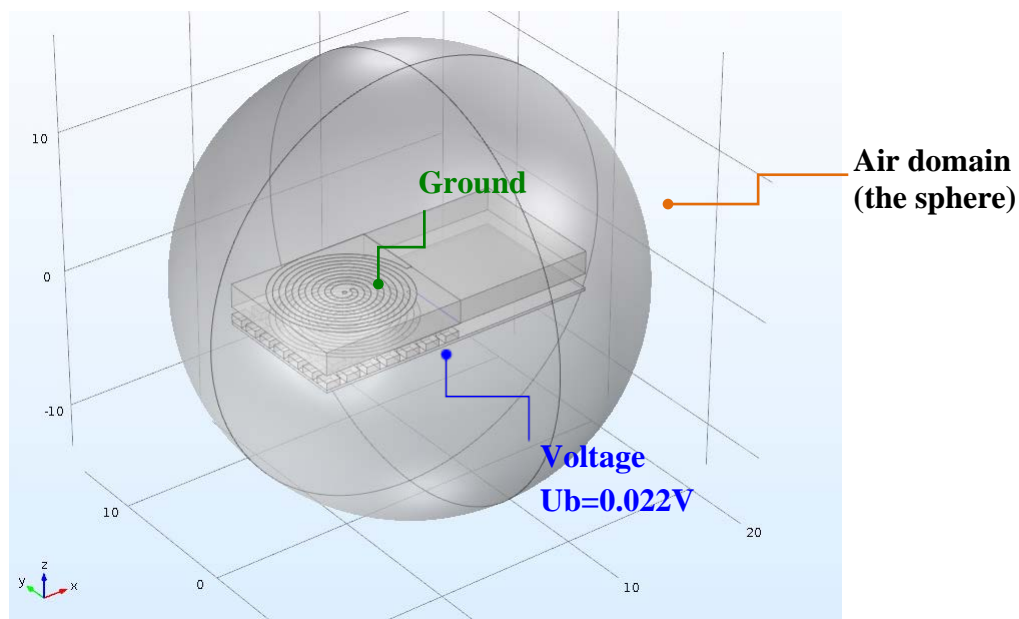
Figure 6. Initial conditions for electromagnetic field problem.

3.4. SOLVING THE ELECTROMAGNETIC FIELD PROBLEM. THE SIMULATED MODEL CONSISTS OF 185563 ITEMS

The next step is represented by the numerical modeling that involves the discretization of the problem with partial derivatives and implicitly its approximation with a problem, which has a solution described by a finite number of degrees of freedom, thus reducing, most often, the solution of the field problem to solving a linear system of algebraic equations or a series of such systems (Fig. 7).

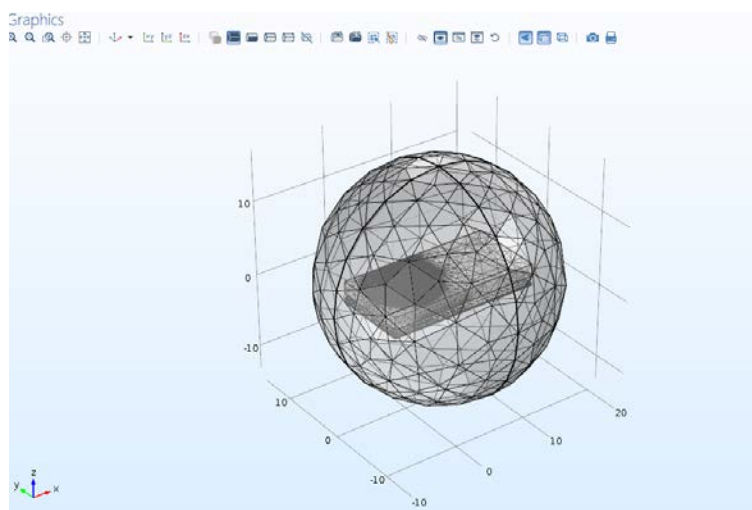The simulated model consists of 185563 tetrahedral elements.

Figure 7. The discretization of the analyzed model in finite elements.

The initial conditions related to the residual magnetization for permanent magnets and the current density for coils according to Figures 8 and 9 are defined. Solving the structural problem also involves a calculation of the electromagnetic force.

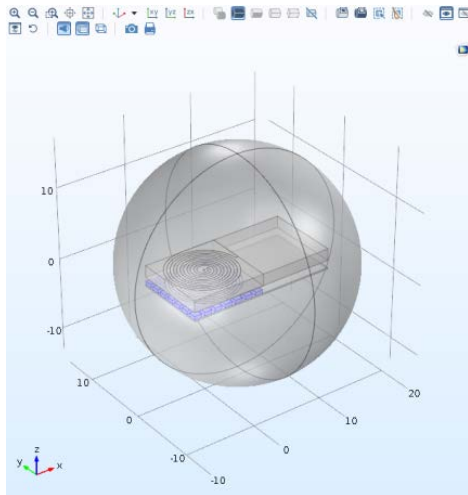$$\mathbf{B} = \mu_0 \mu_r \mathbf{H} + \mathbf{B}_r \qquad (8)$$
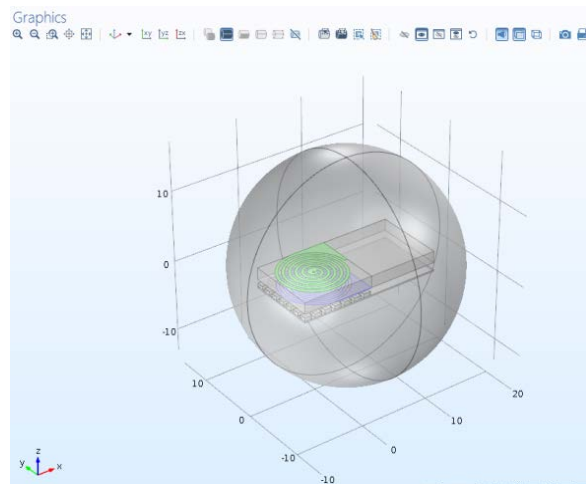
Figure 8. Adding of initial conditions.

Figure 9. Adding the current density.

3.5. POST PROCESSING: SOLVING THE PROBLEM AND DISPLAYING THE RESULTS

The magnetic field problem is solved as it is up mentioned above. The forces acting on the magnets are calculated. Figs. 10 (a, b) and 11 show the magnetic induction spectrum: field lines for two B_r directions, along the Ox axis, respectively, along the Oy axis. The volume density of the forces is calculated from the energy density using the generalized forces theorem (virtual mechanical work) [6, 7].
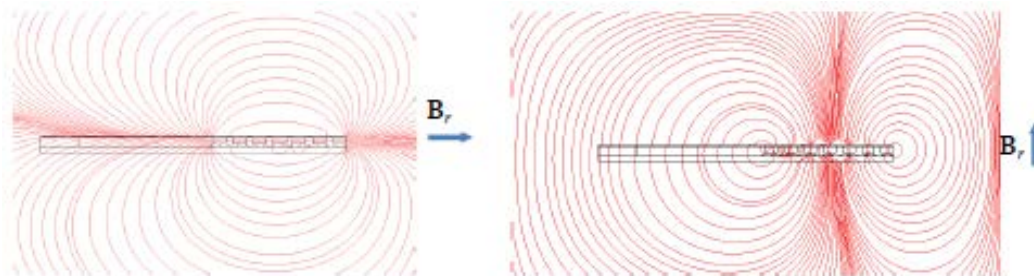
a. Magnetic induction. The maximum value is 1.75 T.   b. Magnetic induction. The maximum value is 2.99 T.

Figure 10. Numerical simulation results for cartesian 2D Model - magnetic induction and deformation. B_r has to be oriented in the direction of Ox [7].
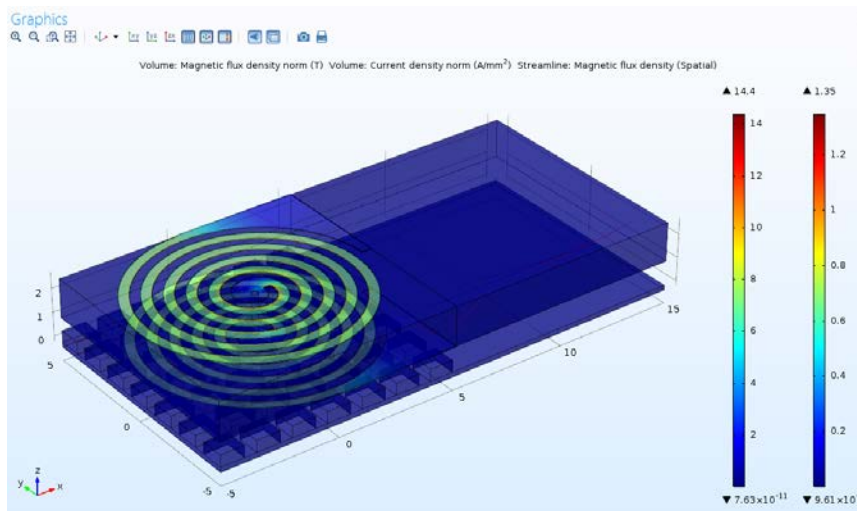

Figure 11. Magnetic induction and 3D model current density with entire blade.

3.6. SOLVING THE STRUCTURAL PROBLEM

Using the magnetic forces calculated after solving the field problem, the structural problem is solved, following the same steps as in the case of the electromagnetic modeling.

In order to solve the mechanical problem, using simplifying elements of geometry and operation, the following steps are involved in the physical, geometric and numerical modeling (Figs. 9 and 10).

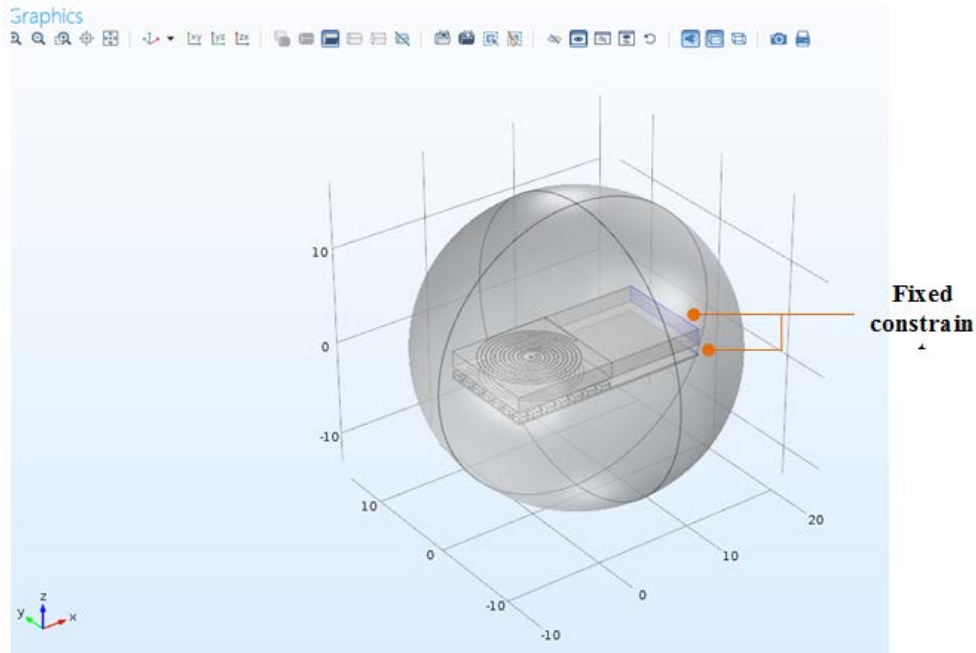### a. Defining the initial conditions for the structural problem

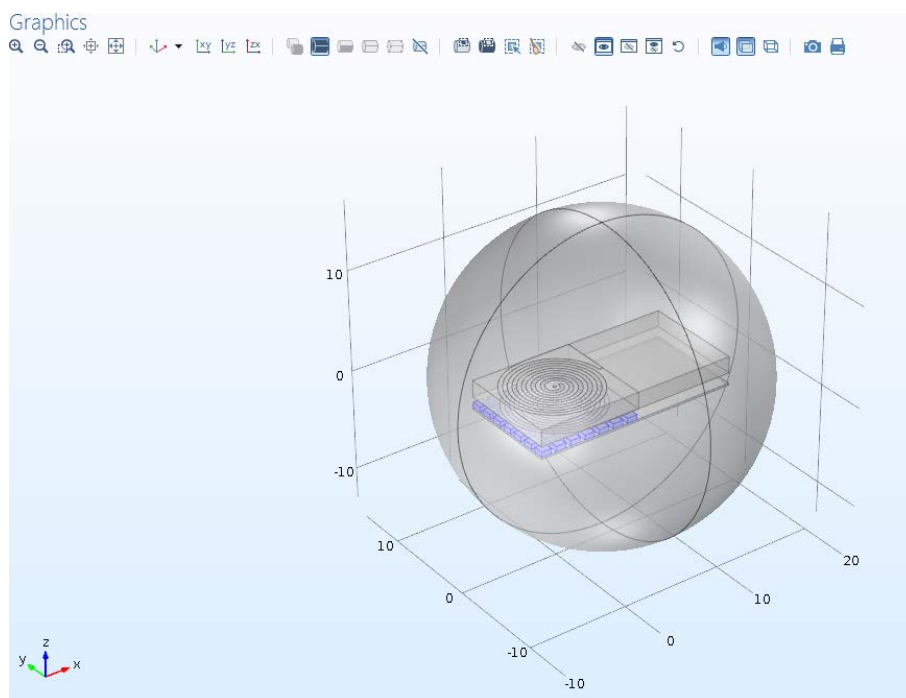**Figure 11. Adding the initial condition Solid Mechanics (solid).**

Figure 12. Adding initial conditions (electromagnetic force).

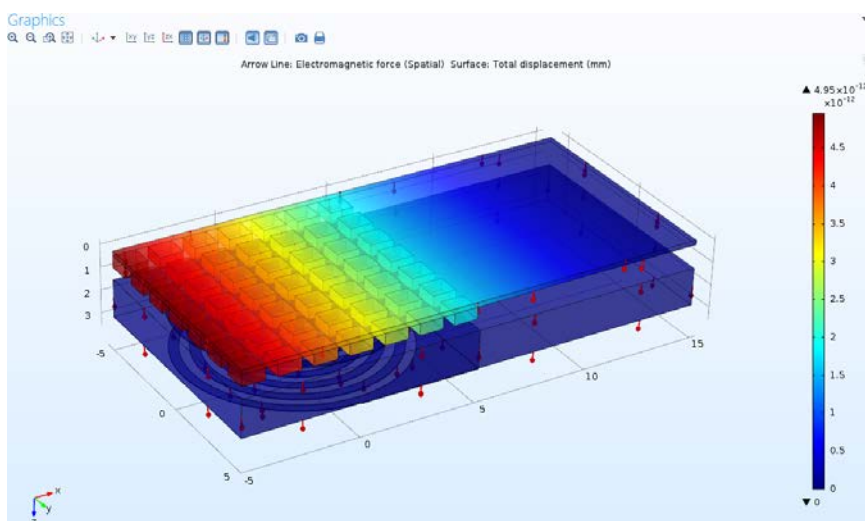*b) Post processing: solving the problem and displaying the results*

Figure 13. Numerical simulation results for blade deformation 3D model.

Figs. 13 and 14 (a, b) shows the deformations determined by numerical simulation. The total force acting on the magnetic matrix is 520.78 N m^{-1}, for **B**r oriented in the direction of *Ox*, and 352.809 N m^{-1} for **B**r oriented in the direction of *Oy*. In these circumstances, the constructive solution to be adopted is the alignment of the magnets with a constant remanent induction oriented horizontally, in the direction of the *Ox* axis (Fig.2.14 a).

a) The magnetic forces raise the PI blade   b) The magnetic forces press the PI blade.
Figure 14. Numerical simulation results [7].

Fig. 15 shows by color maps the deformations for the two actuators, for **B**$_r$ = 1.3 T, and the electric current density **J**n = 5 A mm^{-2}. By comparing the results, 2D modeling can establish an estimation of the actuation in the sense of the order of magnitude.
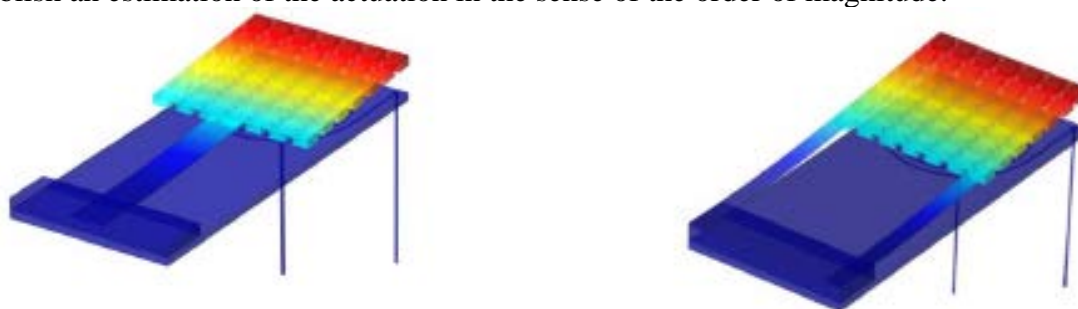
a. The maximum deformation is 1.876 mm.   b. The maximum deformation is 1.280 mm.
Figure 15. Deformations in the stationary operating conditions. [7].

Table 2. The angles of deformations for some analyzed models [6]

Relative permeability, μ_r.	A	B
10	6.45 °	7.02 °
5	12.67 °	13.87 °
2	27.60 °	29.03 °
1	49.06 °	55.81 °

3.7. MODEL ANALYSIS OF DEFORMATIONS AT DIFFERENT FREQUENCIES

In Fig. 16, the deformations of the cantilever and mirror for μ_r = 1, 2, 5, 10, **B**r = 1.3 T, and **J**n = 5 A / mm^2 are presented qualitatively. As expected, the deformations respect the pattern symmetry. However, these may be true for 3D complete models where the PCB coil (printed circuit board) is made of concentric spheres; it is agreeable that the same things can be true when the PCB coil is made of a flat spiral. The entire models with plane spiral coil will be analyzed below.
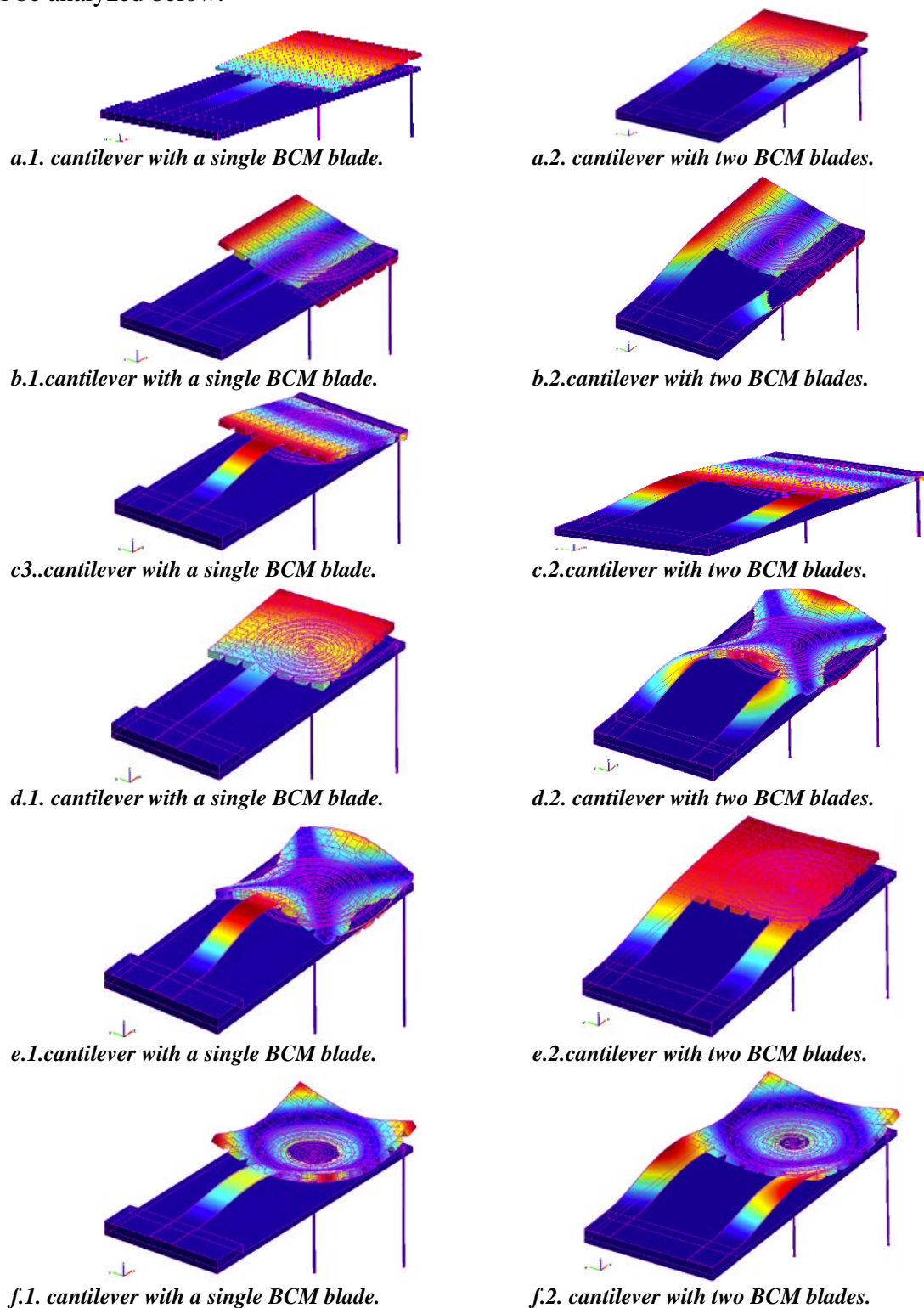

a.1. cantilever with a single BCM blade.   *a.2. cantilever with two BCM blades.*

b.1.cantilever with a single BCM blade.   *b.2.cantilever with two BCM blades.*

c3..cantilever with a single BCM blade.   *c.2.cantilever with two BCM blades.*

d.1. cantilever with a single BCM blade.   *d.2. cantilever with two BCM blades.*

e.1.cantilever with a single BCM blade.   *e.2.cantilever with two BCM blades.*

f.1. cantilever with a single BCM blade.   *f.2. cantilever with two BCM blades.*

Figure 16. Deformations for the six own modes. For one BCM blade, for two BCM blades [7].

As an exception to the first mode, the deformations in all other modes that were considered are more or less removed from the *xOy* symmetry plane. It is then advisable to consider the 3D complete patterns and spiral structure of the PCB coil when the preoccupation is from structural point of view under dynamic conditions.

Table 3. The first six frequencies of the own modes for some analyzed models [6].

Modal frequencies [kHz]	A	B
f_1	0.369	0.295
f_2	3.082	1.059
f_3	5.305	2.884
f_4	8.026	4.471
f_5	49.103	12.512
f_6	49.318	40.462

4. CONCLUSIONS

In order to demonstrate the collaborative work and concurrent engineering, the results of some previous researches were presented in the second part of the paper regarding the numerical simulation of the interactions in the electromagnetic field that take place in two constructive variants of blade console type actuators (beam) with one or two arms in stationary operating conditions. Stationary and structural electromagnetic field (stress-strain) patterns are coupled univocally: electromagnetic forces are input data used in structural analysis.

The results provided by these simulations, carried out as a result of the previous researches, are necessary for design stage, realization and experimentation / operation at optimal parameters without exceeding the resonance frequency of this type of actuator. In this regard, the collaborative work in concurrent engineering was achieved by interconnecting the numerical simulations with the electromechanical design, important parts of the new products realization at optimal operating parameters considering the intended purpose, reducing the costs and the time of realization, this representing an important part in the concurrent engineering.

REFERENCES

1. Bengu, G., *A Computer-Aided Total Quality Approach to Manufacturing Education in Engineering, Topic 3: Concurrent Engineering*, 1996. Available online: http://www.ewh.ieee.org/soc/es/Aug1996/030/cd/en495w03/begin.htm.
2. Parsaei, H.R., Sullivan, W.G., *Concurrent Engineering: Contemporary Issues and Modern Design Tools*, Springer US, 1993.

3. Lagorce, L.K. et. al., *IEEE J. Microelectromech. Syst.*, **8**(1), 2, 1999.
4. Dutoit, B.M. et.al., *Sensors andActuators,* **77**, 178, 1999.
5. Cugat, O. et. al., *Proc. IEEE MEMS 2000*, 485, 2000.
6. Morega, A.M. et. al., *Proceedings of The 8th International Symposium on Advanced Topics in Electrical Engineering*, 2013.
7. Morega, A.M. et. al., *Proceedings of The 9th International Symposium on Advanced Topics in Electrical Engineering*, 556, 2015.
8. Mocanu, C.I., *Electromagnetic Field Theroy*, 2nd Ed. (in Romanian), Ed. Didactica Pedagogica, Bucharest, 1982.
9. COMSOL A.B. v 3.5a – 5.0.
10. Dutoit, B.M. et. al., *Sensors and Actuators*, **77**, 178, 1999.
11. KATCO, *Performance Materials*, http://www.katco.eu/index.htm
12. http://www.ndfeb-info.com/characteristics.aspx
13. http://www.intemag.com/magnetic_properties.html
14. http://www.mit.edu/~6.777/matprops/polyimide.htm
15. Aksyuk, V.A. et al., *Proc. SPIE*, **4178**, 320, 2000.
16. Pan, Y. et al., *Opt. Lett.*, **26**(24), 1966, 2001.
17. Suciu, G. et al., Proceedings of The 6th CEAS Conference - Aerospace Europe, 1, 2017.